

Catalysis Science & Technology

Accepted Manuscript



This is an *Accepted Manuscript*, which has been through the Royal Society of Chemistry peer review process and has been accepted for publication.

Accepted Manuscripts are published online shortly after acceptance, before technical editing, formatting and proof reading. Using this free service, authors can make their results available to the community, in citable form, before we publish the edited article. We will replace this *Accepted Manuscript* with the edited and formatted *Advance Article* as soon as it is available.

You can find more information about *Accepted Manuscripts* in the [Information for Authors](#).

Please note that technical editing may introduce minor changes to the text and/or graphics, which may alter content. The journal's standard [Terms & Conditions](#) and the [Ethical guidelines](#) still apply. In no event shall the Royal Society of Chemistry be held responsible for any errors or omissions in this *Accepted Manuscript* or any consequences arising from the use of any information it contains.

Amoxidation of 2-methylpyrazine to 2-cyanopyrazine over Nb-V oxides: Marked effect of Nb/V ratio on the catalytic performance

Naresh Dhachapally^{1,2}, V. Narayana Kalevaru^{2*}, Andreas Martin²

¹ Begumpet, Doulthabad, Medak, Andhrapradesh, India-502334

² Leibniz-Institut für Katalyse e.V. an der Universität Rostock, Albert-Einstein-Str. 29a, D-18059 Rostock, Germany

* Email: narayana.kalevaru@catalysis.de; Tel: +49-381-1281284; Fax. +49-381-128151284

Abstract

A series of bulk Nb-V-containing mixed oxide catalysts with varying Nb/V ratios were synthesized and studied by various solid state characterizations. Their catalytic performance was evaluated for the gas phase amoxidation of 2-methylpyrazine (MP) to 2-cyanopyrazine (CP) that showed a growing interest in the chemical industry, recently. The catalysts were characterised by BET-SA, XRD, UV-Vis DRS, FTIR, XPS, and TEM. BET surface area decreased continuously with increase in vanadia content. XRD data confirmed the changes in the crystalline phases with altering Nb/V ratios. UV-Vis DRS and FTIR spectroscopic results showed the formation of various kinds of V-oxide species in the catalysts with change in V-content. An increase in the concentration of vanadium changes the nature of VO_x species from isolated vanadia species to polymeric vanadia species and then to crystalline vanadia species. Among all, the Nb-V-O catalyst with a Nb/V ratio of 1 exhibited the superior performance in the amoxidation reaction (i.e. X-MP ~100% and selectivity to 2-CP ~70%). Additionally, a very high space-time-yield of CP (>440 g_{CP}/kg_{cat}·h) could be successfully achieved. This best catalyst sample revealed two dimensional polymeric V-oxide species. TEM and SEM showed the formation of a rod shaped nanoparticle morphology. XPS data revealed that the vanadium is present in two oxidation states (V⁺⁵ and V⁺⁴) in the fresh catalyst (Nb/V = 1) and only one oxidation state (V⁵⁺) in the spent catalyst.

Key words: Nb-V-O solids; Amoxidation; 2-Methylpyrazine; 2-Cyanopyrazine; Solid state characterization

1 Introduction

The heterogeneously catalyzed ammoxidation of olefins, aromatics and hetero aromatics is an industrially important process for the manufacture of various commercially useful nitriles [e.g. 1]. For instance, 2-cyanopyrazine (CP), which is also prepared by the ammoxidation of 2-methylpyrazine (MP) is a valuable intermediate for the production of pyrazinamide, an effective “anti-tubercular drug” [1-6]. According to a World Health Organization (WHO) report published in 2012 [7], the tuberculosis (TB) remains still an immense global problem. The report claims that there were approximately 8.7 million new cases of TB in 2011 and about 1.4 million deaths across the globe. Geographically, the burden of TB is the highest in Asia and Africa. In fact, India and China together account for about 40% of the world’s TB cases. The Millennium Development Goal of WHO is to prevent the TB epidemic by 2015. In view of this, there is a need for developing new and efficient drugs and drug intermediates (for instance, pyrazinamide and cyanopyrazine fall in this category) to handle the TB problem worldwide.

In general, mixed metal oxide (bulk or supported) catalysts are an important class of catalytic materials that are normally employed in numerous oxidation and ammoxidation studies including large scale industrial applications [e.g. 8-13]. Different catalytic systems have been investigated so far for the ammoxidation of MP to CP, and among them V-based catalysts are found to be the most promising ones [1, 3-6, 14-20]. In addition, FePO₄ [21], MoVPO [16], VPO based solids [22], heteropolyacids [17, 23], VMoO_x [24] and supported catalysts such as V₂O₅/TiO₂ [3, 4, 25] are some of the interesting catalyst systems for the ammoxidation of MP to CP. Furthermore, some other studies were also focused a couple of decades ago on the reaction kinetics using Sb-V-Mn mixed oxides [e.g. 26]. One of the main disadvantages of the reported catalysts [e.g. 3, 6, 16, 17] is that they reveal rather low space-time-yields of CP (STY-CP) and their relatively low stability. Therefore, the development of efficient catalysts for the target reaction is in the focus of the present research.

In the recent past, Nb-containing catalyst systems are also reported to be effective and attractive and hence much attention is being focused on the application of Nb oxides for various selective oxidation reactions [27, 28]. However, niobia itself is a poorly active solid for different catalytic reactions. But the combination of niobium oxide with

other redox components (e.g. vanadium, chromium, molybdenum etc.) could significantly improve both the activity and selectivity of many important oxidation reactions. More particularly, the combination of vanadium and niobium oxides has been found to be highly selective and also active for different oxidation and ammoxidation reactions [14, 29-32]. In this context, the synthesis and application of Nb-V-containing oxide materials for the present ammoxidation of MP to CP could be helpful.

Recently we have observed that bulk metal vanadates are very active and selective for the present MP ammoxidation. Furthermore, these catalytic systems also offer very high STY-CP [33-35]. Particularly, a Nb-V-O catalyst has shown a better performance compared to other metal vanadates in the ammoxidation of MP to CP [33, 34]. The key point to reach high catalytic performance appears to be the ability to tune the catalyst surface and bulk structure by changing different characteristics of the solids. For example, this can be accomplished by optimizing the ratio of active components (i.e. Nb and V) in the catalyst composition.

The main objective of the present study is to prepare various Nb-V-containing mixed oxide catalysts with varying Nb/V ratios and evaluate its impact on the catalytic performance in the gas phase ammoxidation of MP to CP. A further intension of this investigation is also to obtain a comprehensive understanding on the physico-chemical characteristics of the catalyst materials by applying various characterization techniques.

2 Experimental

2.1 Catalyst preparation

The preparation of the bulk Nb-V-O catalysts was carried out in two steps. The 1st step dealt with the preparation of a niobium metal solution using the requisite quantities of ammonium niobium oxalate (ANO) precursor. ANO was dissolved in distilled water, to which a desired amount of citric acid (mole ratio of metal: citric acid = 3: 1) was added and then the mixture was stirred at room temperature until clear solution is obtained. The 2nd step contained the preparation of a vanadium solution using NH_4VO_3 (AMV) as a precursor for vanadium. The required amount of AMV was taken in distilled water and a suitable amount of oxalic acid (OA) was added to it (mole ratio of AMV: OA = 1: 1.5). The above solution was then heated to 60 °C on a hotplate and then kept the solution at the same temperature for 10 minutes under stirring. The vanadium solution turned to a

dark blue color after the addition of oxalic acid. Afterwards, the above vanadium-oxalic acid solution was added drop wise to the niobium-citric acid solution at 60 °C under constant stirring. After complete addition, the mixture was heated to 80 °C and then slowly evaporated to dryness on a hotplate. The solid thus obtained was further dried at 110 °C for 16 h in an oven. Finally, the samples were calcined at 500 °C for 12 h in air (4 l/h). Using the same procedure, a series of Nb-V-O solids was prepared with varying Nb/V ratios in the range from 0.9/0.1 to 0.1/0.9. Additionally, pure V₂O₅ was prepared by the direct calcination of AMV precursor at 500 °C for 4 h in air (4 l/h). Similarly, the pure Nb₂O₅ was also prepared by the direct calcination of ANO precursor at 500 °C for 4 h in air (4 l/h). The sample denotation and the Nb/V ratios are given in Table 1.

2.2 Catalyst characterization

The X-ray diffraction (XRD) patterns were obtained on a X-ray diffractometer STADIP (Stoe, Darmstadt, Germany) using Ni-filtered CuK_α radiation ($\lambda = 1.5418 \text{ \AA}$). The crystalline phases were identified by referring to the ASTM data files.

The pore size distribution (PSD) and surface areas (BET-SA) of the catalysts were determined on NOVA 4200e instrument by N₂-physisorption at -196 °C. Prior to the measurements, the known amount of catalyst was evacuated for 2 h at 200 °C to remove physically adsorbed water. The pore size distribution (PSD) was calculated by BJH methodology using the data from desorption branch. We have taken 49 points in total for this measurement (i.e. 25 adsorption and 24 de-sorption points) in the P/Po range of 0.05 to 0.98. All these parameters were calculated using the software “NovaWin version 11.03” provided by Quantachrome Instruments.

Scanning Electron Microscopy (SEM) measurements were performed using a JSM-7401F apparatus (Jeol) with 1.0 nm resolution at an accelerating voltage of 15 kV. To prepare samples for SEM, samples were adsorbed on a silicon wafer and allowed to dry in air overnight. Transmission electron microscopy (TEM) analysis was made by a JEM-2100F (Jeol) high resolution transmission electron microscope (HRTEM) at a voltage of 200 kV. The catalyst was suspended in ethanol medium by ultra sonication at room temperature for 10 min. A drop of the suspension was placed on a carbon-coated copper grid. After drying the grid, the sample was inserted in the TEM instrument for analysis.

The UV-Vis diffuse reflectance spectra (DRS) were recorded on an Avaspec-2048 (Avantes) instrument using solid probe. For the correction of baseline BaSO₄ (spectroscopic grade) was used as a reference material.

FTIR spectra were recorded on by a Bruker Alpha spectrometer (IFS 66) using solid probe. For these experiments, the catalyst powder was pressed into self-supporting discs (50 mg, Ø 20 mm). Before the measurement, the samples were pre-treated or dehydrated by heating in helium up to 400 °C for 10 min and then cooled down to room temperature followed by evacuation. Generally, the spent samples were also degassed before measurements.

The X-ray photoelectron spectroscopic (XPS) measurements were done with a VG ESCALAB 220iXL unit using MgK_α radiation (E = 1253.6 eV) at a base pressure of the UHV chamber. The C1s binding energy (BE) of 284.6 eV was used as a reference for determining the binding energies.

2.3 Catalytic tests

The catalytic tests were performed in a down flow fixed bed stainless steel reactor (i.d. = 9.4 mm, length = 250 mm) in vapor phase at atmospheric pressure. In a typical experiment, 1 g of the catalyst particles (0.5-0.8 mm size) diluted with equal amount of corundum (catalyst: corundum = 1: 1 w/w) having the same size were loaded into the reactor. The catalyst was packed between two quartz wool plugs in the middle of the reactor. Also the upper and lower portions of the catalyst bed were filled with corundum. The liquid feed of premixed MP and H₂O mixture (mole ratio of MP: H₂O = 1: 13) was metered using a HPLC pump. The liquid was vaporized in a preheating zone. The flow rates of gases such as NH₃, air and N₂ were controlled by mass flow controllers. These gases were taken from commercially available compressed gas cylinders (Air Liquide). The molar ratio of reactant feed mixture was set to MP: H₂O: NH₃: air: N₂ = 1: 13: 7: 26: 22. The reaction was carried out at in the temperature range of 360-400 °C; GHSV = 9500 h⁻¹ and τ = 0.37 s. Two thermocouples were positioned, one at the center of the catalyst bed to indicate the reaction temperature and the other one was attached to the furnace through temperature indicator cum controller to steer the temperature of the reactor. The product samples were collected every hour under steady state conditions and analyzed off-line by gas chromatograph (GC-2014 Shimadzu, Japan) equipped with

a flame ionization detector (FID). The liquid samples were analyzed using FFAP column, while the gaseous products (i.e. CO and CO₂) were also analyzed by the same GC using methanizer and GSQ column.

Conversion (X-MP) of MP, yield (Y-CP) and selectivity (S-CP) of CP were calculated by the following formulas:

$$X - MP = \frac{\text{number of moles of MP reacted}}{\text{number of moles of MP fed}} \times 100\%$$

$$Y - CP = \frac{\text{number of moles of CP formed}}{\text{number of moles of MP fed}} \times 100\%$$

$$S - CP = \frac{\text{number of moles of CP formed}}{\text{number of moles of MP reacted}} \times 100\%$$

The yield and selectivity of the main byproducts pyrazinamide and pyrazine as well as carbon oxides were calculated in the same way. The space-time-yield of CP (STY-CP) was calculated using the following equation:

$$STY - CP = \frac{CP \text{ formed } [g / h]}{catalyst \text{ amount } [kg]}$$

3. Results and Discussion

3.1 XRD

The XRD patterns of the fresh catalysts with varying Nb/V mole ratios are depicted in Fig. 1. The lattice parameters are presented in Table 2. The obtained patterns clearly showed that the type of crystalline phase formed depends strongly on the Nb/V ratio applied [29-31]. The XRD reflections of the as-synthesized niobia (sample 1Nb0VO) at $2\theta = 22.60, 28.58, 36.70, 46.23$ and 50.67° clearly point to crystalline Nb₂O₅ phase, as expected. It is known from the literature that niobia crystallizes in several phases [36, 37] and the pattern found in the present case was very similar to that of the TT-phase of Nb₂O₅ (JCPDS-ICDD file 27-1312), which is reported to be stable up to 700 °C. In the present study, 500 °C is the calcination temperature used and hence the TT-phase should be stable in these samples. Sample 0Nb1VO showed reflections at $2\theta = 15.39, 21.31$ (100 %), $21.74, 26.20, 30.07, 32.43$ and 34.36° , which is a typical pattern of V₂O₅

phase (JCPDS-ICDD file 86-2248, Shcherbinaite). The other samples exhibit patterns that correspond well to various Nb-V-O mixed oxides. Besides Nb₂O₅ phase, sample 9Nb1VO revealed reflections caused by the Nb-rich Nb₁₈V₄O₅₅ mixed-oxide phase (JCPDS-ICDD file 46-0087). The XRD pattern of sample 3Nb1VO showed a single phase of Nb₁₈V₄O₅₅ mixed-oxide with peaks at $2\theta = 20.11, 22.38$ (100 %), 26.21 and 29.70°, which is approximately balanced by the stoichiometry used for the preparation of this sample. The XRD data of sample 1Nb1VO showed major peaks at $2\theta = 14.90, 19.69, 20.54, 21.90$ (100 %), 25.53 and 25.94° pointing to the formation of NbVO₅ mixed oxide phase (JCPDS-ICDD file 46-0046). However, besides the formation of NbVO₅, a very small amount of Nb₁₈V₄O₅₅ (shoulder peak at $2\theta = 22^\circ$) was still detected in this solid. In addition, very weak reflections belonging to V₂O₅ are already observed at $2\theta = 15.37, 20.29$ and 26.15°. The XRD pattern of sample 1Nb3VO mainly showed crystalline V₂O₅ (JCPDS-ICDD file 86-2248, Shcherbinaite) due to the higher concentration of vanadium in this sample. However, a couple of weak reflections corresponding to crystalline NbVO₅ were also still detected at $2\theta = 14.90$ and ~26°. Due to the much higher vanadium proportion, the sample 1Nb9VO exclusively revealed the formation of crystalline V₂O₅; no reflections of any mixed Nb-V-O phase or pure Nb₂O₅ could be seen.

Furthermore, the XRD patterns of the spent catalysts were found to be similar to those of the fresh catalysts; therefore, they are not shown here. This result implies that the catalysts are quite stable during the course of the reaction with respect to their phase composition.

3.2 BET-surface areas, adsorption isotherms and pore size distribution

The specific surface areas of the studied oxide catalysts are displayed in Table 3. The surface area of pure Nb₂O₅ (sample 1Nb0VO) is 86 m²/g while the surface area of pure V₂O₅ (sample 0Nb1VO) is only 4 m²/g. However, a drastic drop in the surface area is observed with the decrease in Nb/V ratio (i.e. increase in vanadium content) of the solids up to sample 1Nb1VO and then this decrease is not much affected with further increase in V-content due to increased concentration of vanadia, which has low surface area. This obviously demonstrates that the vanadium ions might be increasingly blocking the pores of niobium oxide, probably they are occupying interstitial positions of

the host matrix or less porous phases are formed. The latter is supported by the above discussed XRD analyses. The pore volumes are also observed to obey the same trend as that of surface areas. Surface areas of the spent samples were also measured (see Table 3). Their surface areas were found to be marginally decreased compared to those of the fresh catalysts pointing again to only small changes. Furthermore, the average pore size estimated in both the fresh and spent samples is also presented in Table 3.

The adsorption isotherms of both the fresh and spent Nb-V-O catalysts are given in Figs. 2A and B. One can notice that the nature of adsorption isotherm in sample-a (pure Nb_2O_5) is of type IV and V, which is typical for mesoporous solids [38, 39]. With increasing vanadium content, the hysteresis shapes are changing from types IV and V to II and III types, which belong to non-porous solids. Such phenomenon is also evidenced from the drastic decrease in their surface areas when V-content is increased (see Table 3). It can be concluded that the pore structure of the catalysts is changing from mesoporous to non-porous as a function of vanadium content. The hysteresis of 0Nb1VO looks like an almost straight line, indicating its non-porous nature. Consequently, this solid exhibited the lowest surface area. The isotherms of the spent catalysts (Fig. 2B) appeared almost similar pointing to no significant pore structure change during the course of the reaction.

The pore size distributions of both fresh and spent Nb-V-O catalysts with varying Nb/V ratios are shown in Figs. 3A and B. Obviously, all samples revealed unimodal pore size distribution. Sample 1Nb0VO showed a sharp and high intense peak at around 2.7 nm pointing to the exclusive presence of mesopores. After incorporation of certain amount of vanadium, the dominant pore diameter of sample 9Nb1VO moved slightly towards higher pore range, i.e. at 4 nm. At the same time, the intensity of the pore volume curve is also decreased considerably in comparison with the vanadium-free solid proving a considerably changed pore structure and surface area due to the already discussed effects of vanadium introduction. From the Fig. 3A one can also notice that the pore diameter of the other samples with further increasing vanadium content is shifted to higher values and thereby decrease the surface area of the solids dramatically. In the catalysts having higher V-contents the pore structure of catalysts seemed to be almost collapsed and such catalysts show a similar behavior as that of pure V_2O_5 showing just straight line. The pore size distribution of the spent catalysts

(Fig. 3B) is found to be similar to their corresponding fresh catalysts; the intensity of the pore volume curve is decreased slightly and hence their surface areas are a little bit decreased. The pore volumes and pore diameters of Nb-V-O oxide catalysts are given in Table. 3.

3.3 SEM and TEM

The SEM image of sample 1Nb1VO (Fig. 4A) clearly shows the formation of bundles of rod shaped Nb-V-O small particles. From the image, one can also see (inset) the rods with several hundreds of nanometer length. A TEM image is presented in Fig. 4B clearly showing the formation of rod-shaped and also some needle like nanoparticles in the catalyst. The rod-shaped nanoparticles seem to be major in proportion, which are more likely related to NbVO₅ phase, while the small proportion of needle like morphology that is typical for V₂O₅ nanoparticles.

3.4 UV-Vis DRS

The UV-vis diffuse reflectance spectra of fresh and spent samples recorded at room temperature are presented in Figs. 5A and B. The LMCT (ligand-to-metal charge transfer) bands are a sensitive indicator for the vanadium coordination and the degree of polymerization of the vanadium species. The local structures of the V⁵⁺ cations are often associated with the band positions of the LMCT transitions. In the literature, many research groups have studied thoroughly the CT band energies of vanadia based catalysts and these are lying in between 200-570 nm. CT bands lying in between 420-560 nm regions are characteristic for crystalline VO_x species in distorted octahedral environment while the bands in the range from 270-400 nm regions are characteristic for oligomeric tetrahedral coordination of V⁵⁺ ions. The bands around 412 nm region are specific for square pyramidal V⁵⁺ ions and the bands appeared <300 nm are typical for CT transitions of isolated (monomeric) tetrahedrally coordinated V⁵⁺ ions and also V⁴⁺ and V³⁺ ions [40, 41]. Generally, CT transitions are more intense than the d-d transitions in metal oxides.

The measured spectra of the present samples showed three broad absorption bands in the range from 550-420, 420-270 and below 270 nm. Sample 1Nb0VO showed only two band maxima at 330 and 260 nm, which belong to the LMCT transitions of pure

Nb_2O_5 . Similarly, all other samples of the present study exhibited three absorption bands with band maxima at 235, 340 and 480 nm (see Fig. 5A). In sample 9Nb1VO, only polymeric (330 nm) and isolated VO_x species (235 nm) of V^{5+} ion bands were clearly observed, which are due to the highly dispersed nature of VO_x species (due to the presence of low vanadium content). However, the band intensities increased with increase in vanadium content. The bands in sample 0Nb1VO correspond well to the CT transitions of V^{5+} ions (i.e. pure V_2O_5). The spectra of samples from 3Nb1VO to 1Nb9VO with increasing vanadium content have shown bands that are quite similar to those of pure V_2O_5 , however, the band positions and energies are quite different to bulk V_2O_5 . The transition energies of vanadium ions are also found to vary with Nb/V ratio of the catalyst. It seems that the metal incorporation plays an important role on the structure in the formation of different nature and coordination environments of VO_x species. Such changes in the nature of VO_x species formed are also expected to exhibit clear impact on the catalytic performance.

The spectra of the spent catalysts are very similar to the fresh ones. This could be assigned to the stability of the crystalline phases that seem to be not altered during the course of the reaction. These results are well correlated with the results obtained by phase and texture analysis.

3.5 FTIR spectra

The FTIR spectra of fresh Nb-V mixed oxide solids are shown in Fig. 6A. Pure vanadia (0Nb1VO) and niobia (1Nb0VO) reveal the well-known spectra and are not shown here. V_2O_5 generally exhibits two characteristic bands, one at ca. 1020 cm^{-1} , (stretching vibrations of $\text{V}^{+5}=\text{O}$ bonds) and a second broad one at ca. 835 cm^{-1} (V–O–V deformation vibrations). Nb_2O_5 shows four broad bands at ca. 850, 725, 635 and 500 cm^{-1} . These bands can be assigned to Nb=O in highly distorted NbO_6 groups, symmetric stretching of the niobium polyhedra, and ν (Nb–O) in slightly distorted NbO_6 octahedra, respectively.

The spectrum of sample 9Nb1VO exhibits various bands at 1020, 975, 885, 735, 575 and 475 cm^{-1} . The bands at 885, 735, 575 and 475 cm^{-1} can be assigned to the Nb_2O_5 matrix. The band at 1020 cm^{-1} is due to the stretching vibrations of the V=O bonds, probably belonging to microcrystalline V_2O_5 that is present in the sample, even at such a

low vanadium content [12, 32, 42]. As expected, the intensity of this band is increasing significantly with increase in V-content of the catalysts. Another band observed at 975 cm^{-1} could be assigned to the two-dimensional amorphous vanadium oxide species present in the system. This band has also been correlated with the vibrations of isolated V=O bands of the type VO^{2+} . Moreover, the band at 975 cm^{-1} may also be due to bulk V=O functionality of crystalline $\text{Nb}_{18}\text{V}_4\text{O}_{55}$ phase. When the vanadium content increases, the band becomes broadened and shifts to lower frequencies, which indicates a weakening of the $(\text{V}=\text{O})^{3+}$ bonding coincident with an amorphous oxide phase or the presence of neighboring V^{4+} ions. Interestingly, the band at 975 cm^{-1} is almost disappeared at higher vanadium contents, which means the bulk V_2O_5 portion has also increased, and perhaps this band is overlapped by the intense and relatively broad band appeared at 1005 cm^{-1} . In addition, the band at 885 cm^{-1} also vanished, which is due to the decline of the niobia proportion. The band appeared at 1005 cm^{-1} is certainly due to stretching vibrations of V=O bands for V_2O_5 [13], while the band at 815 cm^{-1} is due to bending vibrations of V-O-V groups in NbVO_5 (asymmetric stretching of VO_4^{3-} entity). The broadening of these bands with vanadia loading indicates a stronger interaction between vanadia and niobium species. Furthermore, the formation of the orthovanadate phases at higher loadings may be due to the interaction of the isolated vanadate species with the host matrix. These results are in good agreement with the literature reports [12, 32, 41] revealing that the stabilization of vanadate species depends on the nature of acid–base properties of host matrix and also on the vanadia concentration. No considerable differences could be noticed between the fresh and spent samples again; thus, the spectra of the spent samples were not included.

3.6 XPS

The Nb $3d_{5/2}$ BEs of the best (fresh and spent) sample 1Nb1VO (206.9 and 207.3 eV, respectively) are given in Table 4. This region is assigned to Nb^{5+} ions matching well with the data reported in the literature [43, 44]. XP Spectra of the fresh and spent (the best) 1Nb1VO catalyst is given in Fig. 7. The V $2p_{3/2}$ spectra of fresh catalyst can be fitted into two components [45, 46]. The one at higher binding energy (518.0 eV) is assigned to V^{5+} sites. The second peak, at lower binding energy (516.6 eV) can be related to the presence of certain amount of V^{4+} species in the near-surface-region.

Amarilla et al. [44] also claimed the formation of V^{4+} species (about 25%) in $NbVO_5$ being isostructural to monophosphate tungsten bronzes. However, in the used catalyst, only V^{5+} (BE = 517.4 eV) ions were detected. The O1s spectra showed a peak at around 530.1 eV, which is attributed to the O^{2-} ion in $NbVO_5$. In addition to the main peak, a very small shoulder appeared at 533.2 eV in the spectra and the contribution of this peak is only less than 5%. The weak peak might be related to the oxygen attached to lattice or surface defects in the $NbVO_5$ structure [47]. However in the spent catalyst, only a single type of oxygen species was observed.

The nominal value of atomic ratio of Nb/V in this catalyst is 1. Interestingly, the Nb/V ratio in the near-surface-region is found to be different. The fresh catalyst exhibits a Nb/V ratio of 0.79, while the spent catalyst displays 0.62 (see Table 4). In any case, there is a clear enrichment of vanadium in the near-surface-region compared to its bulk value. Such enrichment is more pronounced in case of spent catalyst. This fact shows that reaction conditions have shown a certain influence on the migration of V-species from the bulk to the surface during the course of the reaction. Nonetheless, no considerable difference in the bulk Nb/V ratio (estimated from ICP) could be noticed between the fresh and spent catalyst.

3.7 Catalytic results

The effect of the reaction temperature on the conversion of MP (X-MP), yield of CP (Y-CP) and selectivity to CP (S-CP) is displayed in Figs. 7A-C. The conversion of MP is increased with increase in temperature from 360 °C to 380 °C where nearly the total conversion is reached in most cases and hence it remained more or less constant at this level with further rise in temperature to 400 °C. As expected, the sample 1Nb0VO exhibited a very low activity (X-MP \leq 20%) and selectivity (S-CP \sim 5%) at any given reaction temperature. Pyrazine (Py) was the main by product while pyrazinamide (PyA), small amounts of CO, and CO₂ were the other by products of the reaction. Even though the pyrazinamide is formed, it is also a desired product with good commercial application as anti-tuberculosis drug. In fact, the formed major product CP is also ultimately converted to Py-A by catalytic hydration on industrial scale in the direction of preparing anti-tuberculosis drug formulations. In general, the selectivity of CP increased with temperature up to 380 °C and then slightly decreased with further increase in

temperature. Similarly, the yield of CP also increased (Fig. 7B) with temperature up to 380 °C and then decreased. The best results were obtained over the sample with a Nb/V ratio = 1.

The influence of the Nb/V ratio on the catalytic performance of the solids at 380 °C is shown in Fig. 8. Pure Nb₂O₅ is very less active and not selective for the formation of CP. It can be easily seen that the presence of vanadium shows a remarkable influence on the catalytic performance with respect to the desired reaction. Therefore, both the conversion of MP and the selectivity of CP depend strongly on the Nb/V ratio of the catalysts. In sample 9Nb1VO, Y-CP reaches only 22% while the yield for pyrazine climbs to 52%. The yield of CP passes through a maximum (Y-CP is close to 70%) over 1Nb1VO sample with increased vanadium content. However, a further increase in vanadium content reveals an adverse effect despite the conversion maintains high. The obtained yield of CP over pure V₂O₅ was only 54% (0Nb1VO). In addition, the results clearly showed that the sum of the yields of both CP and PyA accounts to nearly 90 % using sample 1Nb1VO whereas increasing or decreasing vanadium content promotes the formation of unwanted by-products. Large amounts of pyrazine are formed using catalysts with niobium excess and total oxidation is dominant with increasing vanadium proportion. From these results, it is very clear that the ratio of Nb/V ratio has a strong influence on the catalytic performance. Consequently, one can notice that the Nb-V-O catalysts, with a Nb/V ratio of 1 (NbVO₅) exhibits the best performance compared to other solids of this series.

Furthermore, the STY-CP (see Fig. 8) is also increased with an increase in the vanadia content up to a Nb/V ratio of 1 (440 g_{CP}/kg_{cat}·h). After reaching this maximum, the STY-CP drops again down to ca. 350 g_{CP}/kg_{cat}·h for pure V₂O₅. However, the aggregated STY for CP plus PyA might reach ca. 600 g_{CP+PyA}/kg_{cat}·h, this is much higher than the reported literature up to now. The better catalytic performance of Nb-V-O catalysts particularly with a Nb:V ratio of 1:1 (i.e. 1Nb1VO catalyst) is more likely due to the presence of higher concentration of NbVO₅ phase in this formulation compared to all other solids having either high niobium or high vanadium contents. At higher content of Nb, more Nb-oxide or mixed oxide (Nb₁₈V₄O₅₅) phases are present while at high vanadium contents mainly V₂O₅ is present. Both these situations and phase composition seem to be not suitable for achieving enhanced catalytic performance. Usually, when

V_2O_5 phase is formed, the lattice oxygen is connected through $V^{5+}-O-V^{5+}$ bonds, where it is very easy to remove such lattice oxygen due to the high reducibility of the two V^{5+} ions, which in turn leads to easy combustion of MP and thus reduced selectivity of desired product, CP. On the other hand, when metal vanadate is formed (e.g. $NbVO_5$ in the present case), the lattice oxygen is present in $V^{5+}-O-M^{n+}$ bonds ($M=Nb$ in the present case) instead of $V^{5+}-O-V^{5+}$ bonds as present in V_2O_5 phase. This situation leads to lower concentration of $V^{5+}-O-V^{5+}$ bonds and hence low combustion activity of the catalyst compared to V_2O_5 . In other words, the high selectivity of 1Nb1VO catalyst is a result of the fact that the oxide is made up of isolated VO_4 units that are separated from each other by NbO_x units in such a way that all the lattice oxygen ions are located in the solid bridge between V^{5+} and Nb^{+5} ions. Our results are in good agreement with the literature reports that deal with various metal vanadates and claim similar such observations like us [48-50]. Another reason for the improved performance of 1Nb1VO catalyst is due to enrichment of both vanadium and niobium species in the near-surface-region, as evidenced by XPS (see Table 4). The nominal value of Nb : V bulk ratio in the as synthesized catalyst is 0.5 : 0.5 (i.e. 1 : 1). However, XPS analysis revealed that the fresh catalyst exhibit a Nb : V ratio of 0.79 : 1 in the near-surface-region, while the spent catalyst displays a Nb : V ratio of 0.62 : 1. Nevertheless, further studies are certainly necessary to get deeper insights on deriving structure-activity relationships.

Herein we discuss some important issues related to the nature of active sites required, structure-activity relationships as well as mechanistic aspects reported in the literature using different catalyst systems for the present ammoxidation reaction. Hong et al. [16] applied MOVPO catalysts and claimed that the ammoxidation of MP proceeds through a series of dehydrogenation and oxidation steps to form various intermediates such as pyrazinyl aldehyde and pyrazinyl carboxylic acid, which then finally converted into CP. Due to the involvement of dehydrogenation and oxidation steps, the authors suggest that the catalyst should contain both dehydrogenation sites as well as oxygen supply units in appropriate amounts. V_2O_5 is the main active component in MoVPO catalyst for oxygen supply, however pure V_2O_5 also has too strong activity of oxygen supply and only a few sites of dehydrogenation. As a result, it promotes over oxidation of MP and thereby low selectivity of CP. In order to minimize the combustion activity of bulk V_2O_5 , they have added P as a promoter so that it can react with V_2O_5 and form

(VO)₂P₂O₇ and/or α - or β -VOPO₄ phases. In these catalysts, V=O is considered to be the site of oxygen supply, and V⁴⁺ or V⁴⁺-P-O is the site of dehydrogenation. The addition of MoO₃ strengthens the ability of oxygen supply as it can connect with V to increase the fluidity of electron and weaken the bond energy of V=O. The authors state that this situation can also change the space structure between sites of dehydrogenation and oxygen supply. Addition of TiO₂ can further stabilize V⁴⁺, keep the proper V⁴⁺/V⁵⁺ ratio, and can also make VO_x species more dispersed on the surface of the catalyst [51]. A conversion of MP ~95% and S-CP of ca. 75% are reported over these catalysts. Bondareva et al. [15] applied phosphorus modified V₂O₅-TiO₂ catalysts for the ammoxidation of MP and reported that the content of P in the total catalyst plays a key role on the performance. The active sites of the samples with a low concentration of phosphorus contain V⁵⁺ cations in a strongly distorted octahedral oxygen environment, which are strongly bound to a support due to the formation of V-O-Ti bonds. The catalytic properties of the samples containing high P₂O₅ content (10 wt%) are due to the presence of a triple V-P-Ti compound with an atomic ratio of V:P:Ti is nearly 1:1:1. The V⁵⁺ cations in this compound with high P content are present in a weakly distorted tetrahedral oxygen environment and are bound to the tetrahedral P⁵⁺ cations. The authors studied two regions of compositions such as the catalysts with a low (<5wt% P₂O₅) and high (>10wt% P₂O₅) contents of the P additive. The low content of P increases the activity, while the high content of P decreases both the activity as well as selectivity of the desired product, accompanied by a simultaneous increase in the selectivities of by-products such as pyrazine and carbon oxides. On the other hand, addition of alkali promoters, e.g. Na or K modified V₂O₅/TiO₂ catalysts in MP ammoxidation, showed a reduced activity and selectivity of the catalysts due to formation of bronzes (e.g. MV₆O₁₅) and vanadates (e.g. α -NaVO₃, K₃V₅O₁₄ etc.) [25]. However, the active sites of these modified samples are reported to be similar to those in the binary V-Ti-O catalysts, i.e. V⁵⁺ cations strongly bound to TiO₂ and located in a distorted octahedral oxygen environment. The higher the content and basicity of the additive, the more pronounced is the decrease in the V/Ti ratio and the activity. In another study, Bondareva et al. [3] investigated the mechanism of ammoxidation of MP by in-situ FTIR and described that the interaction of methylpyrazine with catalyst surface involves a consecutive transformation of coordinatively bound methylpyrazine into

oxygenated surface compounds, e.g. an aldehyde-like complex and an asymmetrical carboxylate species, which are also coordinatively bound through the nitrogen atom to the surface Lewis acid sites. In the presence of ammonia, such oxy-intermediates further interact with adsorbed ammonia species and form surface amidopyrazine and cyanopyrazine products.

In the last part, we would like to give a brief summary of different catalytic systems applied, reaction conditions, space-time-yields reported by various research groups and compare them with that of the present metal vanadates. For instance, heteropoly acids [e.g. 5], FePO_4 [20] gave a MP conversion of 75-80 %, CP yield of 50 -56 % and STY of only 65-135 $\text{g}_{\text{CP}}/\text{Kg}_{\text{cat}}\cdot\text{h}$. More than 80% yield of CP at 99% conversion of MP were also reported on $\beta\text{-VOPO}_4/\text{SiO}_2$ [52] and VSbPO_x [53] catalysts but the STY of CP achieved over these systems is relatively low, i.e. ca. 110 $\text{g}_{\text{CP}}/\text{Kg}_{\text{cat}}\cdot\text{h}$. One US patent claims 87% conversion of MP, 67% yield of CP with very low STY of CP ($\sim 75 \text{ g}_{\text{CP}}/\text{Kg}_{\text{cat}}\cdot\text{h}$) using multi-component MoPWAIO_x catalyst at high reaction temperature of 440 °C [54]. To the best of our knowledge, the best STY of CP reported so far in the literature is $<150 \text{ g}_{\text{CP}}/\text{Kg}_{\text{cat}}\cdot\text{h}$. On the whole, it can be stated that the present metal vanadate catalysts showed much improved catalytic performance in terms of atom efficiency and space-time-yields of CP.

4. Summary and Conclusions

The results revealed clearly that the Nb/V ratio in NbVO_x solids is indeed an important parameter that needs to be tuned carefully for improving the oxidation properties of solids in a more selective way. The change in Nb/V ratio has shown a substantial influence on physico-chemical characteristics (e.g. porosity, phase composition, crystallinity, nature of VO_x species, reducibility, surface composition, morphology etc.) of the catalysts and thereby catalytic activity and selectivity as well. In the present study, the catalytic properties of Nb-V-O solids were evaluated for the ammoxidation of MP to CP. Surface areas and pore volumes were found to decrease with dropping Nb/V ratio of the solids. Moreover, the type of VO_x species formed and the crystalline phases present in the calcined solids were observed to depend strongly on the content of vanadium (i.e Nb/V ratio) in the catalyst. The XPS analysis exhibited a clear enrichment of vanadium in the near-surface-region in the best catalyst (Nb/V = 1), which appeared

to be responsible for an enhanced selectivity of CP. The catalytic results demonstrated that the ratio of Nb/V in the final catalyst played a key role on the catalytic performance. The results showed that the nature of the vanadium-oxygen sites changed with vanadia content, too. The oligomeric/polymeric vanadia species were considered to be selective for the formation of CP during the ammoxidation of MP. Among all the catalysts tested, the best performance was achieved over the catalyst having an Nb/V ratio of 1 (that corresponds to the NbVO₅ phase). Furthermore, almost total conversion of MP and ca. 70% yield of CP (close to 90% for aggregated yield of CP and PyA) along with extremely high space-time-yield of CP (440 g_{CP}/kg_{cat}.h or 600 g_{CP+PyA}/kg_{cat}.h) was successfully achieved. Finally, the conclusion is that 1Nb1VO (NbVO₅) is the best composition for delivering the high productivity of desired product (CP). This might be due to the involvement of the all Nb⁵⁺ and V⁵⁺ ions in the bond formation of Nb-V-O oxide, and also with surface enrichment of vanadium species as a VO₄³⁻.

Acknowledgements

Thanks are due to Dr. M. Schneider and Dr. J. Radnik both of LIKAT for XRD and XPS measurements.

References

- [1] A. Martin, V.N. Kalevaru, *ChemCatChem*, 2010, **2**, 1504-1522.
- [2] A. Kagarlitskii, L. Krichevskii, A. Amirkhanova, *Pharmaceutical Chem. J.*, 1999, **33**, 381-383.
- [3] V.M. Bondareva, T.V. Andrushkevich, E.A. Paukshtis, N.A. Paukshtis, A.A. Budneva, V.N. Parmon, *J. Mol. Catal. A: Chem*, 2007, **269**, 240-245.
- [4] V.M. Bondareva, T.V. Andrushkevich, O.B. Lapina, A.A. Vlasov, L.S. Dovlitova, *React. Kinet. Catal. Lett.*, 2003, **79**, 165-173.
- [5] N. Lingaiah, K.M. Reddy, P. Nagaraju, P.S. Sai Prasad, I.E. Wachs, *J. Phys. Chem. C*, 2008, **112**, 8294-8300.
- [6] P. Nagaraju, N. Lingaiah, M. Balaraju, P.S. Sai Prasad, *Appl. Catal. A: Gen.*, 2008, **339**, 99-107.
- [7] Global Tuberculosis Report of WHO (2012).
- [8] I.E. Wachs, *Catal. Today*, 2005, **100**, 79-94.
- [9] E. Heracleous, A.A. Lemonidou, *J. Catal.*, 2010, **270**, 67-75.
- [10] G.V. Isaguliantz, I.P. Belomestnykh, *Catal. Today*, 2005, **100**, 441-445.
- [11] J.M. Amarilla, B. Casal, E. Ruiz-Hitzky, *J. Mater. Chem.*, 1996, **6**, 1005-1011.
- [12] Z. Zhao, X. Gao, I.E. Wachs, *J. Phys. Chem. B.*, 2003, **107**, 6333-6342.
- [13] F. Barbieri, D. Cauzzi, F. De Smet, M. Devillers, P. Moggi, G. Predieri, P. Ruiz, *Catal. Today*, 2000, **61**, 353-360.
- [14] J. Holmberg, R. Häggblad, A. Andersson, *J. Catal.*, 2006, **243**, 350-359.
- [15] V.M. Bondareva, T.V. Andrushkevich, O.B. Lapina, D.F. Khabibulin, A.A. Vlasov, L.S. Dovlitova, E.B. Burgina, *Kinet. Catal.*, 2004, **45**, 104-113.
- [16] C. Hong, Y. Li, *Chinese J. Chem. Engg.*, 2006, **14**, 670-675.
- [17] K. Mohan Reddy, N. Lingaiah, K.N. Rao, P. Nagaraju, P.S. Sai Prasad, I. Suryanarayana, *Catal. Lett.*, 2009, **130**, 154-160.
- [18] Ch. Srilakshmi, N. Lingaiah, P. Nagaraju, P.S. Sai Prasad, K.V. Narayana, A. Martin, B. Lücke, *Appl. Catal. A: Gen.*, 2006, **309**, 247-253.
- [19] K.N. Rao, K.M. Reddy, N. Lingaiah, I. Suryanarayana, P.S. Sai Prasad, *Appl. Catal. A: Gen.*, 2006, **300**, 139-146.
- [20] P. Nagaraju, Ch. Srilakshmi, N. Pasha, N. Lingaiah, I. Suryanarayana, P.S. Sai Prasad, *Appl. Catal. A: Gen.*, 2008, **334**, 10-19.

- [21] P. Nagaraju, Ch. Srilakshmi, N. Pasha, N. Lingaiah, I. Suryanarayana, P.S. Sai Prasad, *Appl. Catal. A: Gen.*, 2008, **334**, 10-19.
- [22] B. Manohar, *J. Chem. Pharmaceut. Res.*, 2012, **4**, 2781-2788.
- [23] Ch. Srilakshmi, P. Nagaraju, B. Sreedhar, P.S. Saiprasad, V.N. Kalevaru, B. Lücke, A. Martin, *Catal. Today*, 2009, **141**, 337-343.
- [24] B.M. Reddy, B. Manohar, E.P. Reddy, K.S. Patil, A.V. Ramarao, Ind. Pat. 182 185 A1, 1999 (CSIR, New Delhi, India).
- [25] V.M. Bondareva, T.V. Andrushkevich, O.B. Lapina, A.A. Vlasov, L.S. Dovlitova, E.B. Burgina, *React. Kinet. Catal. Lett.*, 2003, **78**, 355-363.
- [26] L. Forni, *Appl. Catal.*, 1988, **37**, 305-314.
- [27] E. Rojas, M.O. Guerrero-Pérez, M.A. Bañares, *Catal Commun.*, 2009, **10**, 1555-1557.
- [28] M.O. Guerrero-Pérez, M.A. Bañares, *Catal. Today*, 2009, **142**, 245-251.
- [29] C. Lucarelli, P. Moggi, F. Cavani, M. Devillers, *Appl. Catal. A: Gen.*, 2007, **325**, 244-250.
- [30] N. Krins, L. Lepot, R. Cloots, B. Vertruyen, *Solid State Ionics*, 2009, **180**, 848-852.
- [31] N. Ballarini, F. Cavani, C. Cortelli, C. Giunchi, P. Nobili, F. Trifirò, R. Catani, U. Cornaro, *Catal. Today*, 2003, **78**, 353-364.
- [32] A. Polte, H. Langbein, WILEY-VCH Verlag, 1994, pp. 1947-1952.
- [33] N. Dhachapally, V.N. Kalevaru, A. Martin, Eur. Pat. 2428267 A1, 2012 (LIKAT, Rostock, Germany).
- [34] N. Dhachapally, V.N. Kalevaru, J. Radnik, A. Martin, *Chem. Commun.*, 2011, **47**, 8394-8396.
- [35] N. Dhachapally, V.N. Kalevaru, A. Brückner, A. Martin, *Appl. Catal. A: Gen.*, 2012, **443-444**, 111-118.
- [36] A.V. Rosario, E.C. Pereira, *J. Solid State Electrochem.*, 2005, **9**, 665-673.
- [37] Y. Zhao, X. Zhou, L. Ye, S.C.E. Tsang, *Nano Reviews*, 2012, **3**, 17631-17642.
- [38] C. Sangwichien, G.L. Aranovich, M.D. Donohue, *Colloids and Surfaces A Physicochemical and Engineering Aspects*, 2002, **206**, 313-320.
- [39] F. Rouquerol, J. Rouquerol, K. Sing, Adsorption by Powders and Porous Solids Principles, Methodology and Applications, 1999, Academic Press, San Diego, CA

- [40] H. Berndt, A. Martin, A. Brückner, E. Schreier, D. Müller, H. Kosslick, G.U. Wolf, B. Lücke, *J. Catal.*, 2000, **191**, 384-400.
- [41] H. Tian, I.E. Wachs, L.E. Briand, *J. Phys. Chem. B.*, 2005, **109**, 23491-23499.
- [42] Z. Zhao, Y. Yamada, Y. Teng, A. Ueda, K. Nakagawa, T. Kobayashi, *J. Catal.*, 2000, **190**, 215-227.
- [43] N. Kumagai, N. Ikenoya, I. Ishiyama, K. Tanno, *Solid State Ionics*, 1988, **28-30**, 862-867.
- [44] M. Amarilla, B. Casal, J.C. Galvan, E. Ruiz-Hitzky, *Chem. Mater.*, 1992, **4**, 62-67.
- [45] G. Silversmit, D. Depla, H. Poelman, G.B. Marin, R. De Gryse, *J. Electron. Spectroscopy and Related Phenomena*, 2004, **135**, 167-175.
- [46] M. Demeter, M. Neumann, W. Reichelt, *Surf. Sci.*, 2000, **454-456**, 41-44.
- [47] H. Najjar, H. Batis, *Appl. Catal. A: Gen.*, 2010, **383**, 192-201.
- [48] O.S. Owen and H.H. Kung, *J. Catal.*, 1993, **79**, 265-284.
- [49] M.A. Char, D. Patel, M.C. Kung, H.H. Kung, *J. Catal.*, 1987, **105**, 483-498.
- [50] D. Patel, P.J. Andersen, H.H. Kung, *J. Catal.*, 1990, **125**, 132-142.
- [51] G. Centi, *Appl. Catal. A: Gen.*, 1996, **147**, 267-298.
- [52] S. Shimizu, T. Shoji, N. Abe, M. Doba, A. Taguro, A. Iguchi, T. Nakaishi, US 4 778 890 (1988) (*Koei Chemical Co. Ltd., Japan*).
- [53] S. Shimizu, T. Shoji, N. Abe, M. Doba, A. Taguro, A. Iguchi, T. Nakaishi, EP 253 360 B1 (1988) (*Koei Chemical Co. Ltd., Japan*).
- [54] S. Shimizu, T. Shoji, K. Kono, T. Nakaishi, US 4 931 561 (1990) (*Koei Chemical Co. Ltd., Japan*).

Table 1

Sample denotations and Nb/V ratios of various Nb-V-O catalysts

Sample denotation	Catalyst composition Nb/V ratio (mole)
1Nb0VO	1: 0
9Nb1VO	9: 1
3Nb1VO	3: 1
1Nb1VO	1: 1
1Nb3VO	1: 3
1Nb9VO	1: 9
0Nb1VO	0: 1

Table 2

Lattice parameters of various Nb-V-O catalysts

Catalyst	System	d (Å)*	Lattice parameters (Å)			Volume (Å ³)
			a ₀	b ₀	c ₀	
1Nb0VO	Hexagonal	3.93	3.607	-	3.925	44.2
9Nb1VO	Hexagonal	3.93	3.607	-	3.925	-
3Nb1VO	Orthorhombic	3.96	7.939	17.31	17.61	242.0
1Nb1VO	Orthorhombic	4.05	11.86	5.514	6.915	452.4
1Nb3VO	Orthorhombic	4.39	11.5	4.369	3.557	-
1Nb9VO	Orthorhombic	4.39	11.5	4.369	3.557	-
0Nb1VO	Orthorhombic	4.39	11.5	4.369	3.557	178.8

*100% peak

Table 3

BET surface areas and pore volumes of the Nb-V-O catalysts with varying Nb/V ratios

Catalyst	Surface area		Pore volume		Average pore size	
	(m ² /g)		(ml/g)		(nm)	
	Fresh	Spent	Fresh	Spent	Fresh	Spent
1Nb0VO	86	-	0.193	-	2.7	-
9Nb1VO	39	37	0.139	0.138	3.7	3.4
3Nb1VO	16	13	0.101	0.098	10.7	10.5
1Nb1VO	8	7	0.088	0.060	18	20
1Nb3VO	7	6	0.060	0.050	> 20	> 20
1Nb9VO	6	8	0.047	0.048	> 20	> 20
0Nb1VO	4	-	0.049	-	> 20	> 20

Table 4

XPS results of the best (fresh and spent) Nb-V-O catalyst with Nb/V = 1

Catalyst 1Nb1VO	Nb ⁵⁺		V ⁵⁺		V ⁴⁺		O		O		Nb/V ratio*
	BE (eV)	at.%	BE (eV)	at.%	BE (eV)	at.%	BE (eV)	at.%	BE (eV)	at.%	
Fresh	206.9	8.5	518.0	4.7	516.6	6.1	533.2	2.2	530.1	45.8	0.79
Spent	207.3	11.1	517.4	18.0	-	-	-	-	530.3	60.3	0.62

* near-surface-region

Figure captions

- Fig. 1.** XRD patterns of fresh Nb-V-O catalysts (* = Nb₂O₅ (JCPDS-ICDD file 28-0317); \$ = Nb₁₈V₄O₅₅ (JCPDS-ICDD file 46-0087); § = NbVO₅ (JCPDS-ICDD file 46-0046); # = V₂O₅ (JCPDS-ICDD file 86-2248)) (a – 1Nb0VO, b – 9Nb1VO, c – 3Nb1VO, d – 1Nb1VO, e – 1Nb3VO, f – 1Nb9VO, g – 0Nb1VO)
- Fig. 2.** Adsorption isotherms of various Nb-V-O catalysts (A: fresh catalysts, B: spent catalysts; sample denotation as for Fig. 1)
- Fig. 3.** Pore size distribution of various Nb-V-O catalysts (A: fresh catalysts, B: spent catalysts; sample denotation as for Fig. 1)
- Fig. 4.** Electron microscopy images of 1Nb1VO sample (Nb/V = 1) (A: SEM, B: TEM)
- Fig. 5.** UV-Vis DRS spectra of various Nb-V-O catalysts (A: fresh catalysts, B: spent catalysts; sample denotation as for Fig. 1)
- Fig. 6.** FTIR spectra of various Nb-V-O catalysts (sample denotation as for Fig. 1)
- Fig. 7.** XP Spectra of the best (fresh and spent) 1Nb1VO catalyst (F = Fresh catalyst, U = Used catalyst, sample denotation as for Fig. 1)
- Fig. 8.** Effect of temperature on the catalytic performance of various Nb-V-O catalysts (A: Conversion of MP; B: Yield of CP, C: Selectivity to CP) (Reaction conditions: MP: H₂O: NH₃: air: N₂ = 1: 13: 7: 26: 22; cat. wt. 1g; sample denotation as for Fig. 1)
- Fig. 9.** A comparison of Conversion of MP, product yields and selectivity as well as and space-time-yields of CP obtained over different Nb-V-O catalysts at 380 °C (Reaction conditions: MP: H₂O: NH₃: air: N₂ = 1: 13: 7: 26: 22; cat. wt. 1g; MP = methylpyrazine, CP = cyanopyrazine, Py = pyrazine, PyA = pyrazinamide)

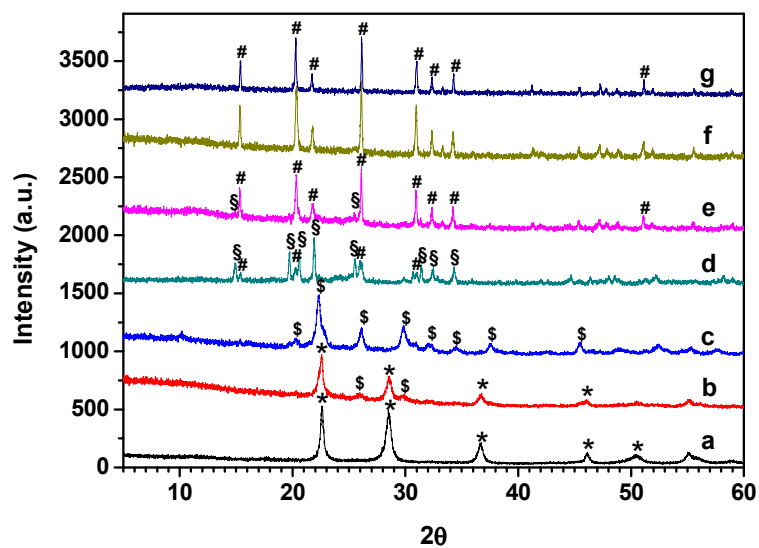
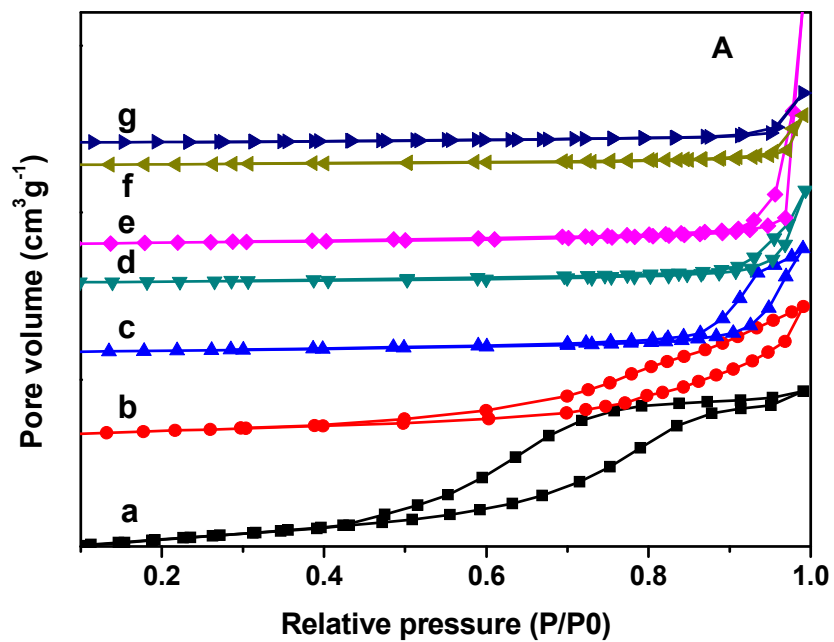
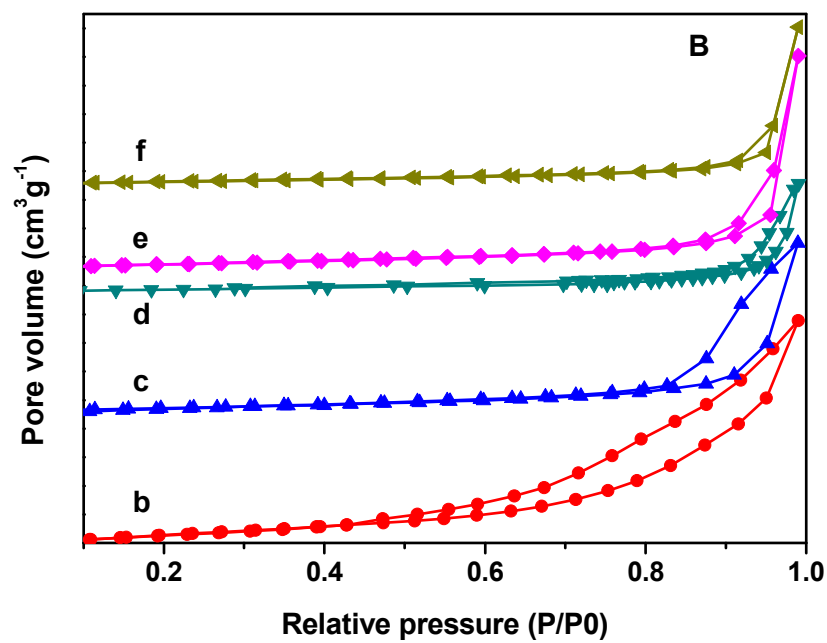
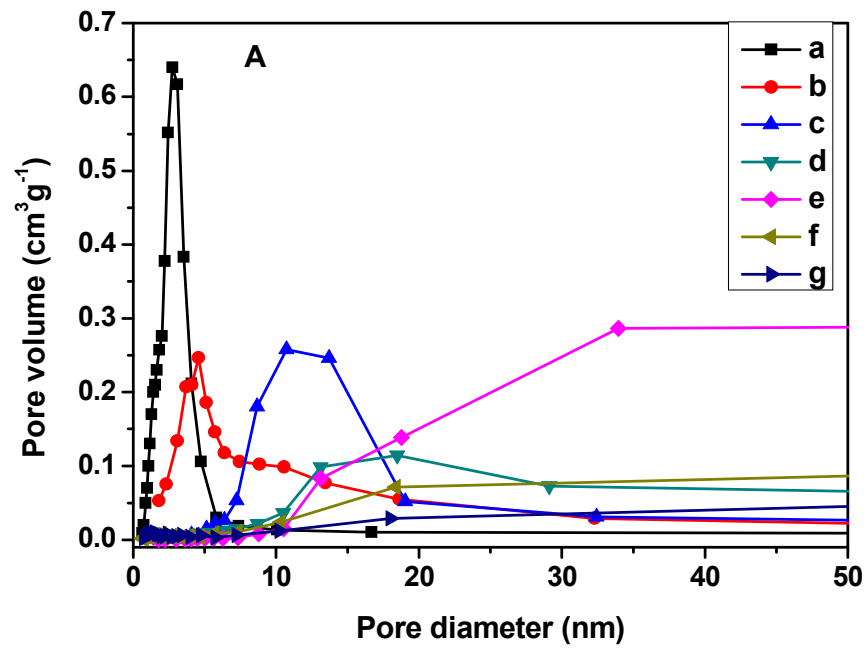


Fig. 1.

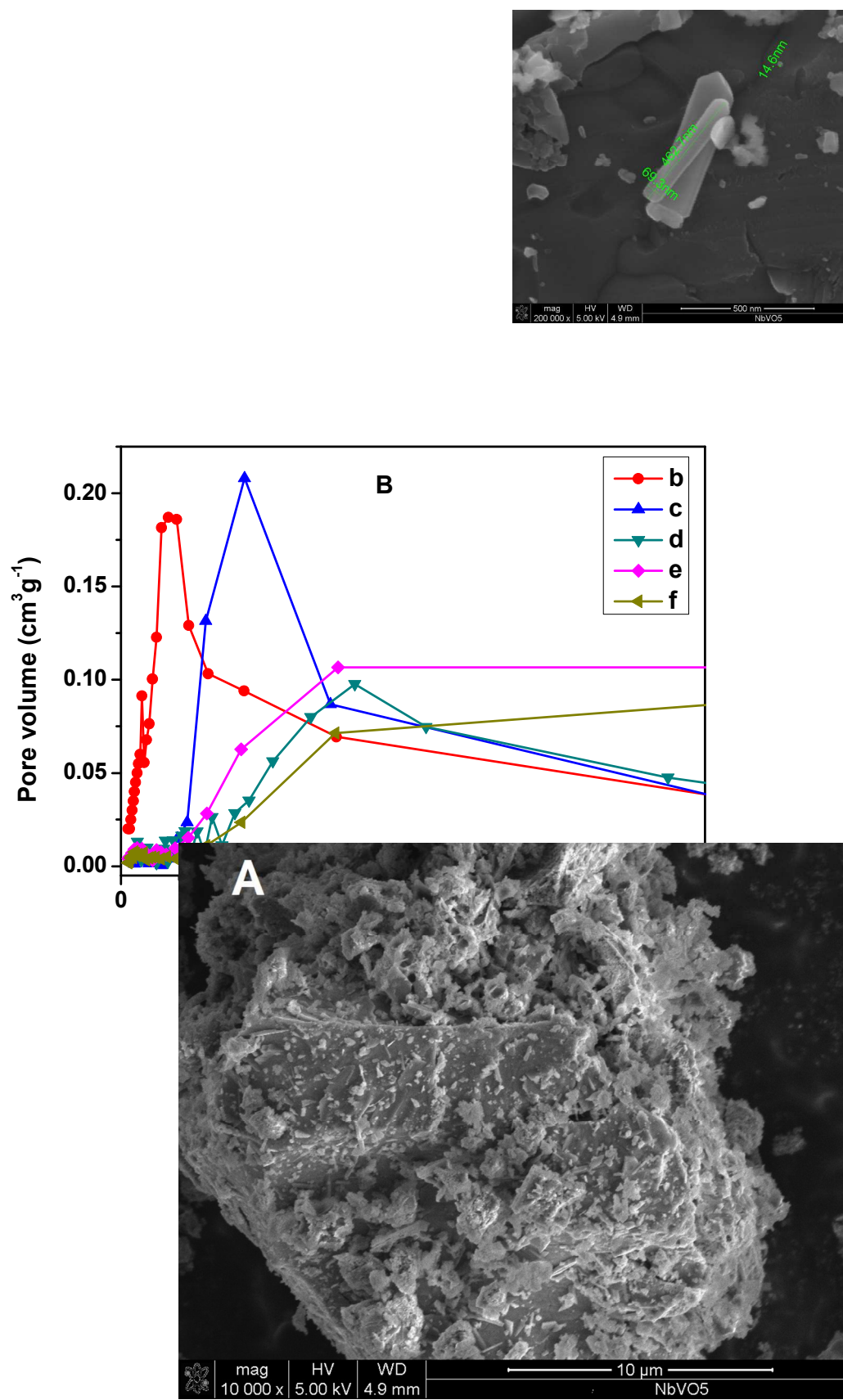


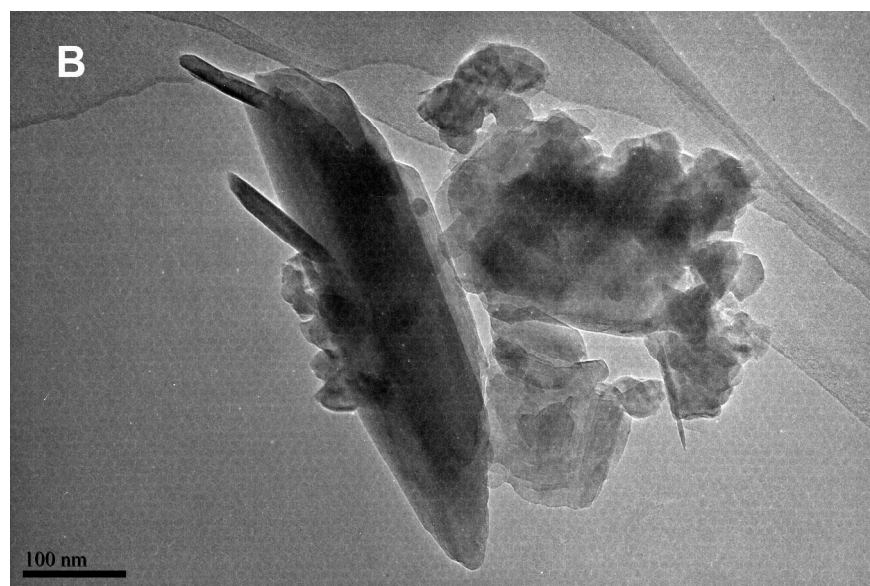


Figs. 2.



Figs. 3.





Figs. 4.

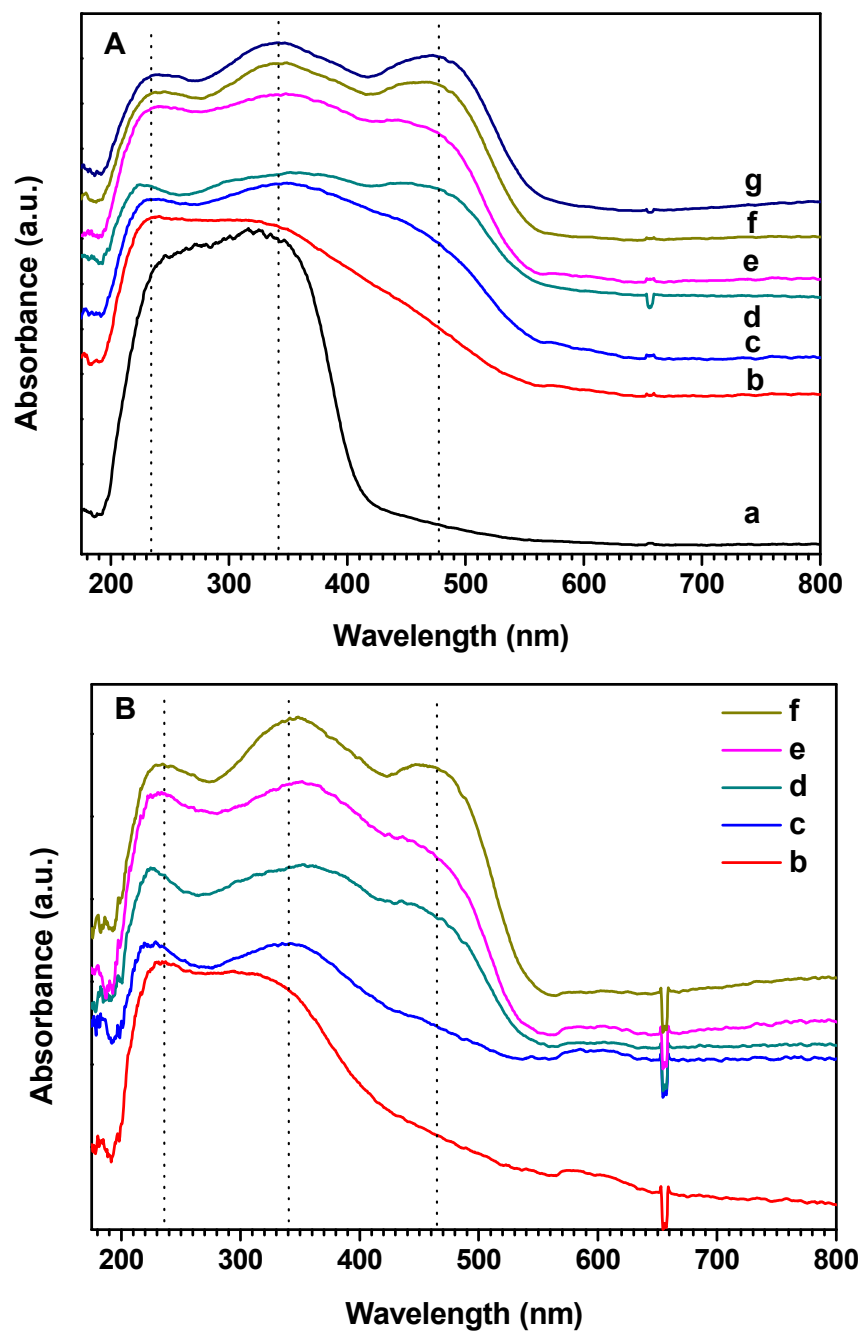


Fig. 5.

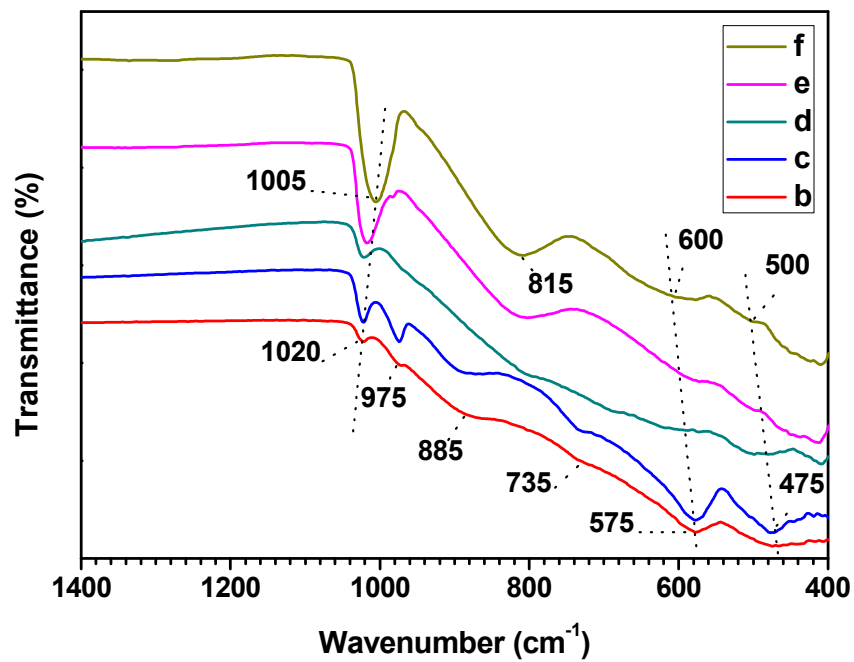


Fig. 6.

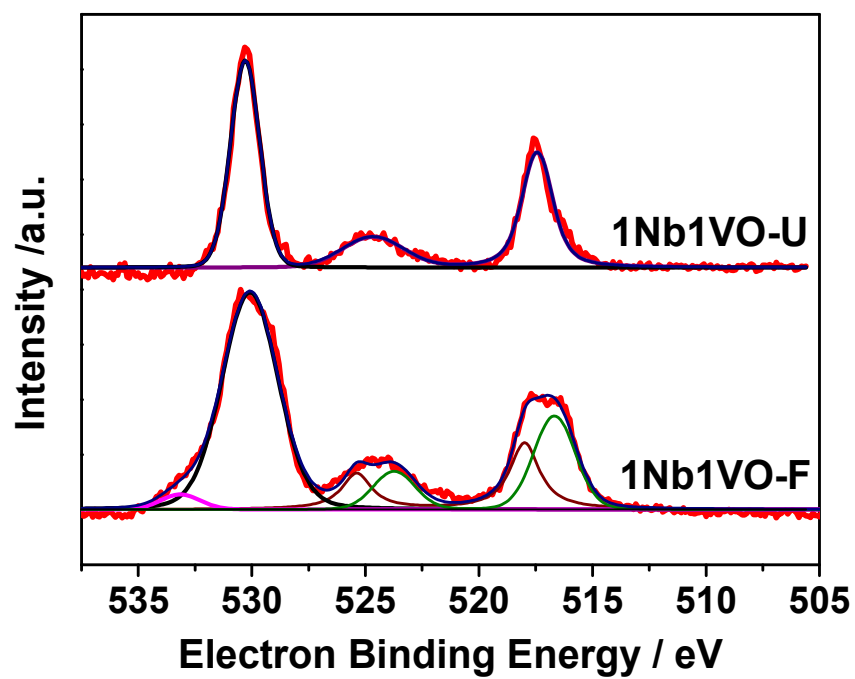
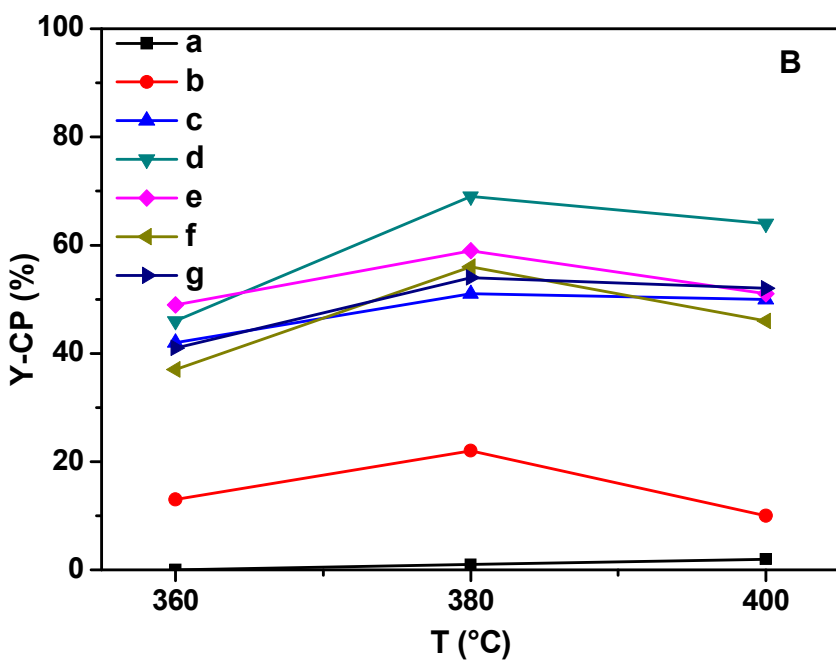
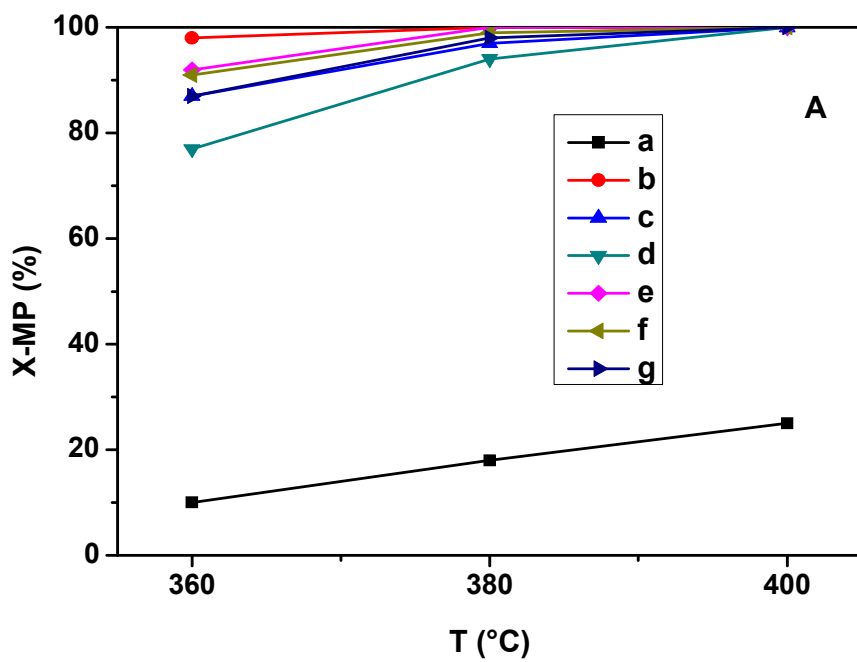


Fig. 7.



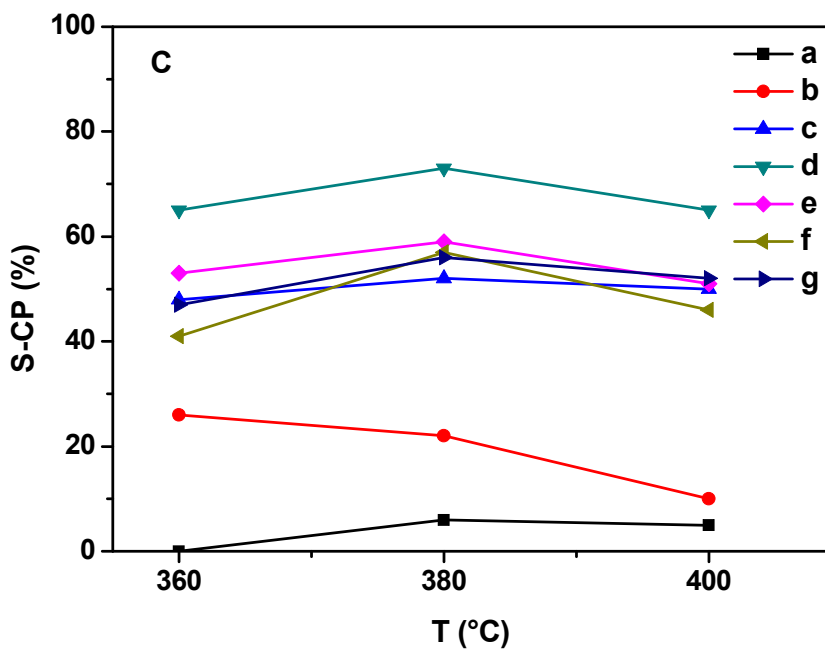


Fig. 8.

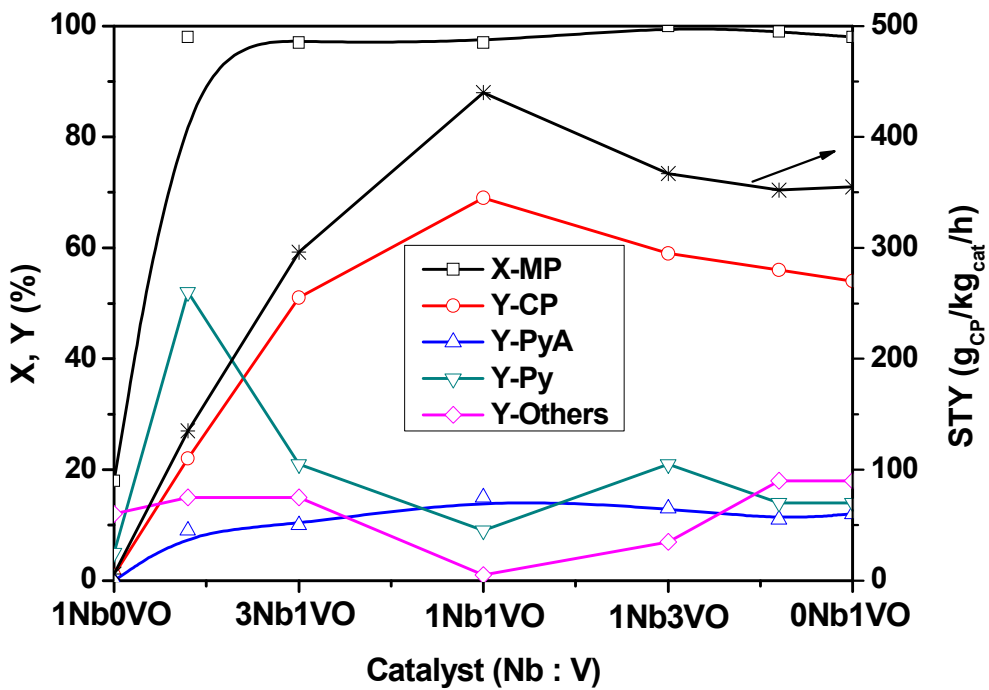
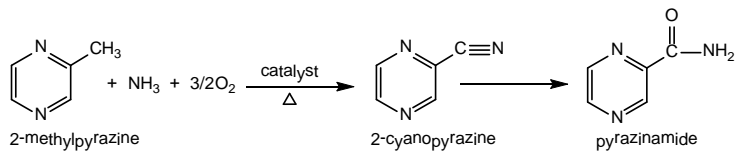
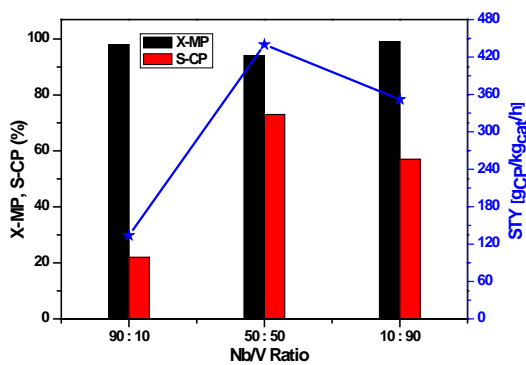


Fig. 9.

Graphic abstract



Among various Nb-V-O catalysts, the catalyst with Nb/V ratio=1 has shown the best activity, selectivity as well as extremely high space-time yields (X-MP ~100%, S-CP~70% and STY=440 g_{CP}/kg_{cat}/h).